The Journal of Immunology
RESEARCH ARTICLE | MARCH 24 2023

Soluble TREM-like Transcript-1 Acts as a Damage-Associated Molecular Pattern through the TLR4/MD2 Pathway Contributing to Immune Dysregulation during Sepsis FREE

Chia-Ming Chang; ... et. al

J Immunol (2023) 210 (9): 1351–1362.
https://doi.org/10.4049/jimmunol.2200222

Soluble TREM-like Transcript-1 Acts as a Damage-Associated Molecular Pattern through the TLR4/MD2 Pathway Contributing to Immune Dysregulation during Sepsis

Chia-Ming Chang,*,[1] Kuang-Hua Cheng,[†,‡,1] Tsai-Yin Wei,[§] Meng-Ping Lu,* Yi-Chen Chen,* and Yen-Ta Lu*,[¶]

Studies have shown that elevated plasma levels of platelet-derived soluble TREM-like transcript-1 (sTLT-1) are associated with an unfavorable outcome in patients with septic shock. However, the underlying molecular mechanisms are not well defined. This research aimed to study the role of sTLT-1 in mediating immune dysfunction during the development of sepsis. Our study demonstrated that patients with septic shock have significantly higher plasma concentrations of sTLT-1, whereas sTLT-1 is not detectable in healthy subjects. Plasma concentrations of sTLT-1 were correlated with the degree of immunosuppressive parameters in monocytes from patients with septic shock. sTLT-1 can first activate monocytes by binding to the TLR4/MD2 complex but subsequently induce immunosuppressive phenotypes in monocytes. Blocking Abs against TLR4 and MD2 led to a significant decrease in sTLT-1–induced activation. Treatment with an anti–TLT-1 Ab also significantly reduces sTLT-1 binding to monocytes and proinflammatory cytokine secretion in a mouse model of endotoxemia. sTLT-1 acts as an endogenous damage-associated molecular pattern molecule, triggering the activation of monocytes through the TLR4/MD2 complex followed by sustained immune suppression. This process plays a crucial role in the development of sepsis-associated pathophysiology. Our findings outline, to our knowledge, a novel pathway whereby platelets counteract immune dynamics against infection through sTLT-1. ***The Journal of Immunology*****, 2023, 210: 1351–1362.**

Sepsis, a systemic inflammatory response syndrome caused by severe infection, remains a global healthcare problem and a life-threatening condition. It is becoming increasingly clear that patients with sepsis exhibit a biphasic immunological response that varies over time. During the initial phase of sepsis, a hyperinflammatory immune reaction is mediated by receptors on innate immune cells capable of responding to a wide range of pathogen- or damage-associated molecular patterns. This acute-phase reaction produces a systemic inflammatory response, including proinflammatory cytokine release, that may cause hemodynamic instability, multiorgan dysfunction, coagulation abnormalities, and shock (1). Concomitant with the hyperinflammatory response is a nearly simultaneous production of anti-inflammatory cytokines; the immune system rapidly enters a hypoinflammatory state (2), manifested as an increased risk of developing late nosocomial infections (2–4). Most patients with sepsis survive the initial hyperinflammatory immune response but cannot survive subsequent secondary infections due to a broadening immune dysregulation (5, 6).

Indicators of the hypoinflammatory state observed in patients with sepsis include lymphocyte abnormalities (2, 4, 7), monocytic deactivation with diminished HLA-DR surface expression, and low TNF-α production (8). Sustained reductions in monocyte HLA-DR expression indicate a high risk for nosocomial infection and death in patients with sepsis (9, 10). Recently, elevated programmed death ligand-1 (PD-L1) expression on monocytes in patients with septic shock was found to be associated with an increased occurrence of nosocomial infections and mortality (11, 12). This finding suggests that the level of PD-L1 expression in monocytes may also serve as a marker for immunosuppression.

Platelets are crucial mediators of hemostasis, but recent advances suggest that platelets can also influence innate and adaptive immune responses (13–15). TREM-like transcript-1 (TLT-1) exists exclusively in the α-granules of resting platelets and on the surface of activated platelets. Upon platelet activation, TLT-1 is quickly exposed to the membrane and subsequently cleaved, leading to the release of a soluble fragment (sTLT-1). High levels of sTLT-1 are significantly correlated with disseminated intravascular coagulation scores (16). Prolonged sTLT-1 expression in the plasma has been associated with reduced survival in patients with septic shock (17). In addition, sTLT-1 has been shown to bind the soluble TREM-1 ligand, thus interfering with leukocyte activation (18). Collectively, these clinical and in vitro studies suggest that sTLT-1 may have multiple effects, playing a role in platelet aggression and mediating leukocyte function during sepsis. However, the physiological function of sTLT-1 is not fully understood. In this study, we specifically investigated the mechanisms by which sTLT-1 interacts with and modulates the host immune system during sepsis.

*Ascendo Biotechnology, Inc., Taipei, Taiwan; [†]Graduate Institute of Clinical Medicine, College of Medicine, National Taiwan University, Taipei, Taiwan; [‡]Department of Critical Care Medicine, MacKay Memorial Hospital, Taipei, Taiwan; [§]Department of Medical Research, MacKay Memorial Hospital, Taipei, Taiwan; and [¶]Chest Division, Medical Department, MacKay Memorial Hospital, Taipei, Taiwan

[1]C.-M.C. and K.-H.C. contributed equally to this work.

ORCIDs: 0000-0001-8166-2011 (K.-H.C.); 0000-0001-5738-2407 (T.-Y.W.); 0000-0003-3056-3026 (M.-P.L.); 0000-0002-9798-8355 (Y.-T.L.).

Received for publication March 28, 2022. Accepted for publication February 27, 2023.

This work was supported by MacKay Memorial Hospital Grants MMH-E-100-08 to MMH-E-109-08.

Address correspondence and reprint requests to Dr. Yen-Ta Lu, 45, Minsheng Road, Tamshui, New Taipei 25160, Taiwan. E-mail address: our0409@gmail.com

The online version of this article contains supplemental material.

Abbreviations used in this article: APACHE II, Acute Physiology and Chronic Health Evaluation II; hTLT-1, human TLT-1; IKKα, IκB kinase α; IQR, interquartile range; MD2, myeloid differentiation factor 2; mTLT-1, murine TLT-1; PD-L1, programmed death ligand-1; rsTLT-1, recombinant soluble TLT-1; SOFA, Sequential Organ Failure Assessment; sTLT-1, soluble TLT-1; TLT-1, TREM-like transcript-1.

Materials and Methods

Study approval

This study was approved by the Institutional Review Board of Mackay Memorial Hospital (Taipei, Taiwan), and written informed consent was obtained from each participant. The procedures of all animal experiments were approved by and complied with the regulations of the Institutional Animal Care and Use Committee of MacKay Memorial Hospital (Taipei, Taiwan).

Clinical sample collection

We enrolled 21 patients with septic shock and 20 healthy subjects in an observational study from April 2013 to April 2014. Septic shock was identified according to the criteria established at the Third International Consensus Definitions for Sepsis and Septic Shock (Sepsis-3) (19). The exclusion criteria included the following: age <20 y, leukemia, and receiving chemotherapy or immunosuppressive therapy. The following clinical and biological data were collected when patients were admitted to an intensive care unit: age, sex, Acute Physiology and Chronic Health Evaluation II (APACHE II) score, and Sequential (sepsis-related) Organ Failure Assessment (SOFA) score. Each blood sample was obtained within 6 h of admission and subjected to the measurement of cell-surface HLA-DR and PD-L1 expression on $CD14^+$ monocytes. Flow cytometric analysis was performed on a BD FACSCalibur flow cytometer (BD Biosciences, San Jose, CA), and the collected data were analyzed using FlowJo software (FlowJo, Ashland, OR). The plasma samples were stored at −80°C until further examination.

Reagents and Abs

AIM-V, DMEM, and RPMI 1640 medium were from Thermo Fisher Scientific (Waltham, MA). *Escherichia coli* LPS strain O111:B4 was purchased from Sigma-Aldrich (St. Louis, MO). Recombinant human TLR4 and MD2 were purchased from R&D Systems (Minneapolis, MN). Phospho-IRF3 (Ser^{396}) (D6O1M) rabbit Ab, phospho−IκB kinase α (IKKα) (Ser^{176}/Ser^{180}) rat Ab, phopho-p38 MAPK (Thr^{180}/Tyr^{182}) (D3F9) rabbit Ab, and phospho-NF-κB p65 (Ser^{536}) (93H1) rabbit Ab were obtained from Cell Signaling Technology (Danvers, MA), and a β-actin Ab was purchased from Proteintech (Rosemont, IL). The anti-MD2 Ab (clone 18H10) was purchased from InvivoGen (Hong Kong, China) and anti-TLR4 Ab (clone HTA125) was purchased from BioLegend (San Diego, CA). Mouse IgG1 (clone MOPC-21 and clone MG1-45) and mouse IgG2a (clone MOPC-173) were from BioLegend. Rat IgG2b (clone LTF-2) and mouse IgG2b (clone MPC-11) were from Bio X Cell (Lebanon, NH). To distinguish cell subsets, FITC-anti-human CD66b (clone G10F5, BioLegend), PerCP-anti-human CD14 (clone MΦP9, BD Biosciences), PerCP-Cy5.5-anti-human CD14 (clone MΦP9, BD Pharmingen), and AF488-anti-human CD14 (clone M5E2, BioLegend) were used to identify granulocytes ($CD66b^{hi}CD14^+$), monocytes ($CD14^{hi}$), and lymphocytes ($CD66b^-CD14^-$). Abs including allophycocyanin-anti-His Ab (clone J095G46, BioLegend), AF647-anti-human TLT-1 (clone 268420, R&D Systems), allophycocyanin-anti-human PD-L1 (clone MIH1, Thermo Fisher Scientific/eBioscience), and BV510-anti-human HLA-DR (clone L243, BioLegend) were used in the detection of markers and recombinant soluble TLT-1 (rsTLT-1) binding on the cell surface. Dead cells were excluded according to fixable viability stain 780 staining (BD Horizon, San Jose, CA). CF647 conjugates of rsTLT-1 and BSA (negative control) were labeled using CF dye and biotin SE (succinimidyl ester) protein labeling kits (Biotium, Fremont, CA)

Generation of rsTLT-1

rsTLT-1 was generated by GenScript (Piscataway, NJ). Briefly, pET30a-rsTLT-1 encoding a human TLT-1 extracellular domain (Gln^{16}–Pro^{162}) with a polyhistidine tag at the N terminus was expressed using *E. coli* and purified using Ni-NTA columns. The purity of the recombinant protein estimated by densitometric analysis of a Coomassie Blue–stained SDS-PAGE gel under reducing conditions was >90%. Endotoxin contamination of the purified proteins was examined using a *Limulus* amebocyte lysate endotoxin assay kit (GenScript). All proteins were sterile, and the endotoxin concentration was lower than the detectable limit (<0.1 endotoxin unit/μg protein).

Preparation of human WBCs and $CD14^+$ monocytes

Human peripheral blood samples from healthy subjects were collected by venipuncture into ACD (acid citrate dextrose) Vacutainer tubes. Human WBCs were separated from peripheral blood using hypotonic erythrocyte lysis in ammonium chloride containing ACK (ammonium-chloride-potassium) solution. Human $CD14^+$ cells were isolated from human PBMCs, which were separated from whole blood through Ficoll-Paque density gradient centrifugation. The selection was carried out with a positive CD14 isolation kit (Miltenyi Biotec, Auburn, CA) following the manufacturer's instructions. The cell viability was >90% according to trypan blue staining.

Flow cytometric analysis

Human rsTLT-1 was added to freshly isolated human WBCs or monocytes in AIM-V medium and cultured at 37°C for 1 h before detection of binding properties using flow cytometric analysis. The Ab-mediated perturbation of rsTLT-1 binding was performed by adding 10 μg/ml Abs to WBCs and culturing them at 37°C for 30 min prior to the rsTLT-1 binding procedures. In some experiments, cells were resuspended in PBS containing 1% FBS at a density of 2×10^6 cells/ml, and nonspecific binding of Abs was blocked by using human Fc Block (BD Biosciences, San Jose, CA) at room temperature for 10 min. Cell surface molecules and rsTLT-1 treatment were examined by incubating cells with primary fluorochrome-labeled Abs at 4°C for 30 min in PBS containing 1% FBS. Subsequent analysis was performed on a CytoFLEX flow cytometer (Beckman Coulter, Indianapolis, IN), and the collected data were analyzed using FlowJo software (FlowJo, Ashland, OR).

Quantitative PCR

Monocytes were cultured in the presence or absence of 10 μg/ml rsTLT-1 for the indicated times. The mRNA from the monocytes was extracted using an RNeasy Plus mini kit (Qiagen, Germantown, MD). The transcripts were processed to cDNA using SuperScript III reverse transcriptase (Invitrogen, Waltham, MA) and quantified using an ABI Prism 7000 sequence detection system (Applied Biosystems, Waltham, MA). The specific predesigned primer/probe sets for TNF-α (Hs00174128_m1), IL-6 (Hs00174131_m1), IL-10 (Hs00174086_m1), and GAPDH (Hs99999905_m1) were purchased from Applied Biosystems.

Western blot

Purified monocytes were stimulated with rsTLT-1 (10 μg/ml) or LPS (100 ng/ml) for the indicated times in AIM-V medium. The cell lysates were resolved using SDS-PAGE and analyzed according to Western blot analysis using various Abs of interest. Signal density was acquired and quantified using a UVP ChemiDoc-It 815 image system (UVP, Upland, CA) and National Institutes of Health ImageJ.

ELISA

Plasma concentrations of sTLT-1 were measured using TREML1/TLT-1 DuoSet ELISA kits according to the manufacturer's instructions (R&D Systems, Minneapolis, MN). In some experiments, monocytes were treated with rsTLT-1 or LPS, and IL-6, IL-10, and TNF-α were then quantified in the culture supernatant by using DuoSet ELISA kits.

Docking analysis of TLT-1 with TLR4 and MD2 proteins

We used the ZDOCK program to illustrate the binding of TLT-1 with the TLR4 and MD2 monomers (20). To identify the binding interactions, the TLT-1 x-ray (PDB ID: 2FRG) (21) and the complexes from the x-ray of

Table I. Demographic and clinical characteristics of patients with septic shock and healthy subjects upon enrollment

	Healthy Subjects (n = 20)	Patients (n = 21)
Age, median (IQR), y	63 (61.3–67.8)	67 (49–74)
Sex, male/female	12/8	10/11
APACHE II score, median (IQR)	NA	25 (19–27)
SOFA score, median (IQR)	NA	11 (9–14)
Site of infection		
Intrapelvic abscess	NA	1
Intravascular catheters	NA	1
Intra-abdominal infection	NA	3
Necrotizing fasciitis	NA	1
Wound infection	NA	1
Pneumonia	NA	9
Peritonitis	NA	1
Infectious diarrhea	NA	1
Urinary tract infection	NA	3
Microbe		
Gram-positive	NA	3
Gram-negative	NA	8
Fungal	NA	1
Mixed infection	NA	5
Unknown	NA	4
28-d mortality	NA	7

APACHE II, Acute Physiology and Chronic Health Evaluation II; IQR, interquartile range; NA, not available; SOFA, Sequential Organ Failure Assessment.

TLR4 and MD2 (PDB ID: 3FXI) (22) were used for the docking procedure. The docking parameters were set to default and with 6° angular sampling. The results generated 186 positions from the program. We selected the best prediction based on the highest ZDOCK score for interaction analysis.

Solid-phase binding assays

We used the solid-phase binding assay to study the direct binding of rsTLT-1 to TLR4 and MD2. Recombinant TLR4 (5 μg/ml in PBS), MD2 (5 μg/ml in PBS), and BSA (negative control) proteins were plated separately in 96-well plates and incubated overnight at 4°C. Blocking buffer (2% BSA in PBS) was added to the plates to avoid nonspecific binding for 2 h at room temperature. Serial dilutions of rsTLT-1 (5–78 ng/ml, 2-fold dilution) were added, and the plates were allowed to incubate at room temperature for 2 h. The anti–TLT-1 Ab (1 μg/ml in PBS) was added for 1 h. Next, the HRP-labeled secondary Ab, anti-rat IgG-HRP, was added to the plate for a 30-min incubation at room temperature. The plates were washed three times with PBS with 0.05% Tween 20 (PBST) between each step. Finally, tetramethylbenzidine substrate was added and the plates were incubated for 10–15 min for detection of the HRP-labeling Ab. After that, 1 N HCl stop solution was added to stop the reaction. Absorbance at OD_{450} was measured by a microplate reader.

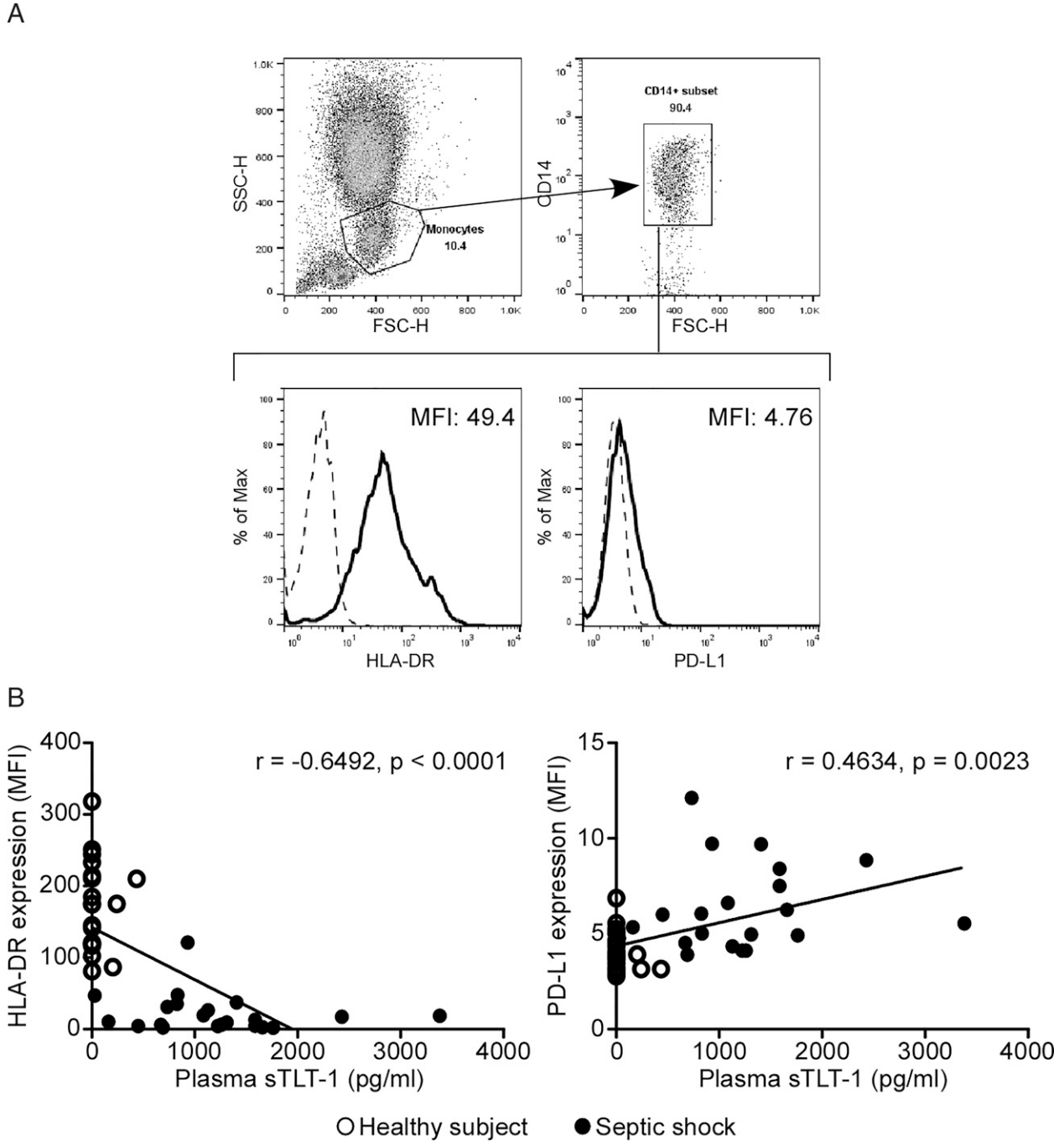

FIGURE 1. Relationship among the levels of plasma sTLT-1, HLA-DR, and PD-L1 expression on monocytes in patients with septic shock. (**A**) Representative gating for monocytes from WBCs is shown. Briefly, monocytes were gated out of all events based on their forward scatter (FSC)/side scatter (SSC) properties, followed by subsequent $CD14^+$ gating. Cells were then identified as $CD14^+$ monocytes. Histograms of geometric mean fluorescence intensity (MFI) of HLA-DR and PD-L1 expressed on monocytes (heavy-line histograms) are shown. Dashed-line histogram represents relative isotype control. (**B**) HLA-DR expression on monocytes was negatively correlated with the level of plasma sTLT-1, whereas a positive relationship was observed between plasma sTLT-1 levels and PD-L1 cell surface expression on monocytes. Correlations were assessed using Pearson's correlation coefficient. Healthy subjects are indicated by an open circle; patients with septic shock are indicated by a closed circle.

THP-1-XBlue-MD2-CD14 cell stimulation assay

The THP-1-XBlue-MD2-CD14 cell line was derived from the human monocytic THP-1 cell line and purchased from InvivoGen (Hong Kong, China). Cells were cultured in RPMI 1640 containing 10% heat-inactivated FBS and antibiotics at 37°C with 5% CO_2. To investigate the effect of anti-TLR4 Ab and anti-MD2 Ab on sTLT-1–induced activation, THP-1-XBlue-MD2-CD14 cells were pretreated with anti-MD2 Ab, anti-TLR4 Ab, or IgG control for 15 min at 37°C with 5% CO_2. After Ab treatment, the cells were treated with rsTLT-1 (10 μg/ml) and incubated for 18 h. Cell culture supernatants were collected for subsequent assessment of cytokine secretion. To assess NF-κB activation, the supernatant of the culture medium was collected, and QUANTI-Blue reagent (InvivoGen) was used according to the manufacturer's instructions. TNF-α was quantified in the culture supernatant by using DuoSet TNF-α ELISA kits.

Stable transfection of human TLT-1 and murine TLT-1 into HEK293 cells

Stable transfection of human TLT-1 (hTLT-1) and murine TLT-1 (mTLT-1) in HEK293 cells (Bioresource Collection and Research Center, Hsinchu, Taiwan) was performed using jetPRIME (PolyPlus, New York, NY) transfection protocols. Briefly, HEK293 cells were cultured in DMEM supplemented with 10% heat-inactivated FBS and 50 IU/ml penicillin and streptomycin at 37°C. The cells were seeded at 4×10^5 cells/well on a six-well plate. The next day, a mixture of jetPRIME reagent and 3 μg of pcDNA 3.1/hTLT-1 or mTLT-1 expression plasmid carrying a neomycin-resistance gene was added to the cells, and the cells were cultured for 24 h. The selection antibiotic G418 (InvivoGen) was added at a concentration of 500 μg/ml, and the culture medium containing the antibiotic was changed every 2–3 d. After 3 wk, the hTLT-1– or mTLT-1– expressing cells were collected using a cell sorter (SH800Z, Sony Biotechnology) to detect cells with high expression and seeded as single cells in each well of a 24-well plate. Cells were maintained in DMEM with 10% heat-inactivated FBS, 50 IU/ml penicillin and streptomycin, and 500 μg/ml G418 at 37°C. hTLT-1 or mTLT-1 expression was analyzed by flow cytometry.

Generation of anti–TLT-1 mAb

Mouse anti–TLT-1 mAbs were generated according to standard protocols as described previously (23). Clone 26A6 was selected in this study due to direct binding to HEK293 cells expressing human or mouse TLT-1 (see Fig. 8A).

The mouse model of endotoxemia

BALB/c mice were purchased from the National Laboratory Animal Center (Taipei, Taiwan) and maintained in the MacKay Memorial Hospital Animal Facility. To determine the protective role of anti–TLT-1 Ab in the endotoxin shock model, female BALB/c mice were i.p. injected with an anti–TLT-1 Ab (5 mg/kg, 26A6) or vehicle (saline) 1 h before or 2 h after LPS injection (5 mg/kg). Peripheral blood plasma was collected from the tail vein, and TNF-α production was measured with a mouse TNF-α ELISA kit (R&D Systems). In survival experiments, BALB/c mice were i.p. injected with lethal LPS (15 mg/kg). One hour before or 2 h after the LPS challenge, mice were injected i.p. with an anti–TLT-1 Ab (20 mg/kg, 26A6) or vehicle (saline) and monitored every 8–12 h.

Statistical analysis

Data were analyzed using Prism 9.0 (GraphPad Software, San Diego, CA) and expressed as the mean ± SEM. Comparisons between groups were performed using a Student *t* test. Correlations were assessed using Pearson's correlation coefficient. A p value <0.05 was considered significant.

Results

Expression of the immunosuppressive phenotypes by HLA-DR and PD-L1 in patients with septic shock are correlated with the increase in plasma concentrations of sTLT-1

This study measured the plasma concentration of sTLT-1 and surface expression of HLA-DR and PD-L1 in 21 patients with septic shock and 20 age-matched healthy subjects. The clinical characteristics of the studied subjects are summarized in Table I. The expression of HLA-DR and PD-L1 on monocytes was analyzed by flow cytometry within 6 h following subject recruitment. The representative gating strategy is shown in Fig. 1A. The plasma concentration of sTLT-1 was measured in each sample using an ELISA kit. Our data showed that the plasma concentrations of sTLT-1 were not detectable in any healthy subjects (median, 0 pg/ml; interquartile range [IQR], 0–0 pg/ml). In contrast, considerably higher plasma sTLT-1 levels were measured in patients with septic shock (median, 1127 pg/ml; IQR, 711–1586 pg/ml, $p < 0.0001$). The expression of HLA-DR on monocytes was significantly lower in patients with septic shock than in healthy subjects (septic shock: median, 13.19; IQR, 4.72–33.25 versus healthy subjects: median, 174.8; IQR, 119.4–213.5, $p < 0.0001$). The expression of PD-L1 on monocytes was significantly higher in patients with septic shock (septic shock: median, 5.54; IQR, 4.65–7.96 versus healthy subjects: median, 3.86; IQR, 3.16–4.63, $p = 0.0002$) (Table II). With speculation that the presence of plasma sTLT-1 may modulate the expression of HLA-DR and PD-L1 on monocytes, the correlation between plasma levels of sTLT-1 with HLA-DR and PD-L1 expression on monocytes was further analyzed. Fig. 1B shows that HLA-DR expression on monocytes was negatively correlated with plasma levels of sTLT-1 ($r = -0.6492$, $p < 0.01$). In contrast, the expression of PD-L1 on monocytes was positively correlated with the plasma levels of sTLT-1 ($r = 0.4634$, $p < 0.01$). These results suggest that the high levels of plasma sTLT-1 observed in patients with septic shock may be an indicator of sepsis-associated immunosuppression.

sTLT-1 induces initial immune activation followed by immunosuppressive phenotype in human monocytes

We then conducted in vitro studies to investigate whether human monocytes from healthy subjects can be induced by sTLT-1 to change immunophenotypes. We incubated freshly isolated human monocytes with rsTLT-1 and examined the expression of HLA-DR and PD-L1 for 3 consecutive days. Parallel groups of human monocytes were compared, with incubation with LPS as a positive control. The representative gating strategy is shown in Fig. 2A. As shown in Fig. 2B (left), HLA-DR expression was significantly upregulated by rsTLT-1 within the first 24 h, followed by a rapid downregulation. PD-L1 expression also increased dramatically within 24 h but remained upregulated throughout the following 3-d experiment (Fig. 2B, right). These data suggest that sTLT-1 alone could induce a biphasic change of immunophenotypes in human monocytes.

To further examine the long-term effects of sTLT-1 on monocytes, we next examined whether rsTLT-1 pretreatment would affect LPS-induced cytokine secretion in human monocytes. First, monocytes were pretreated with rsTLT-1 or LPS. After 48 h, the cells

Table II. Immunological markers of patients with septic shock and of healthy subjects

	Healthy Subjects ($n = 20$)	Patients ($n = 21$)	p
Plasma sTLT-1, median (IQR), pg/ml	0 (0–0)	1127 (711–1586)	<0.0001
HLA-DR, median (IQR), MFI	174.8 (119.4–213.5)	13.19 (4.72–33.25)	<0.0001
PD-L1, median (IQR), MFI	3.86 (3.16–4.63)	5.54 (4.65–7.96)	0.0002

Blood samples were collected within 6 h of admission. IQR, interquartile range; MFI, geometric mean fluorescence intensity.

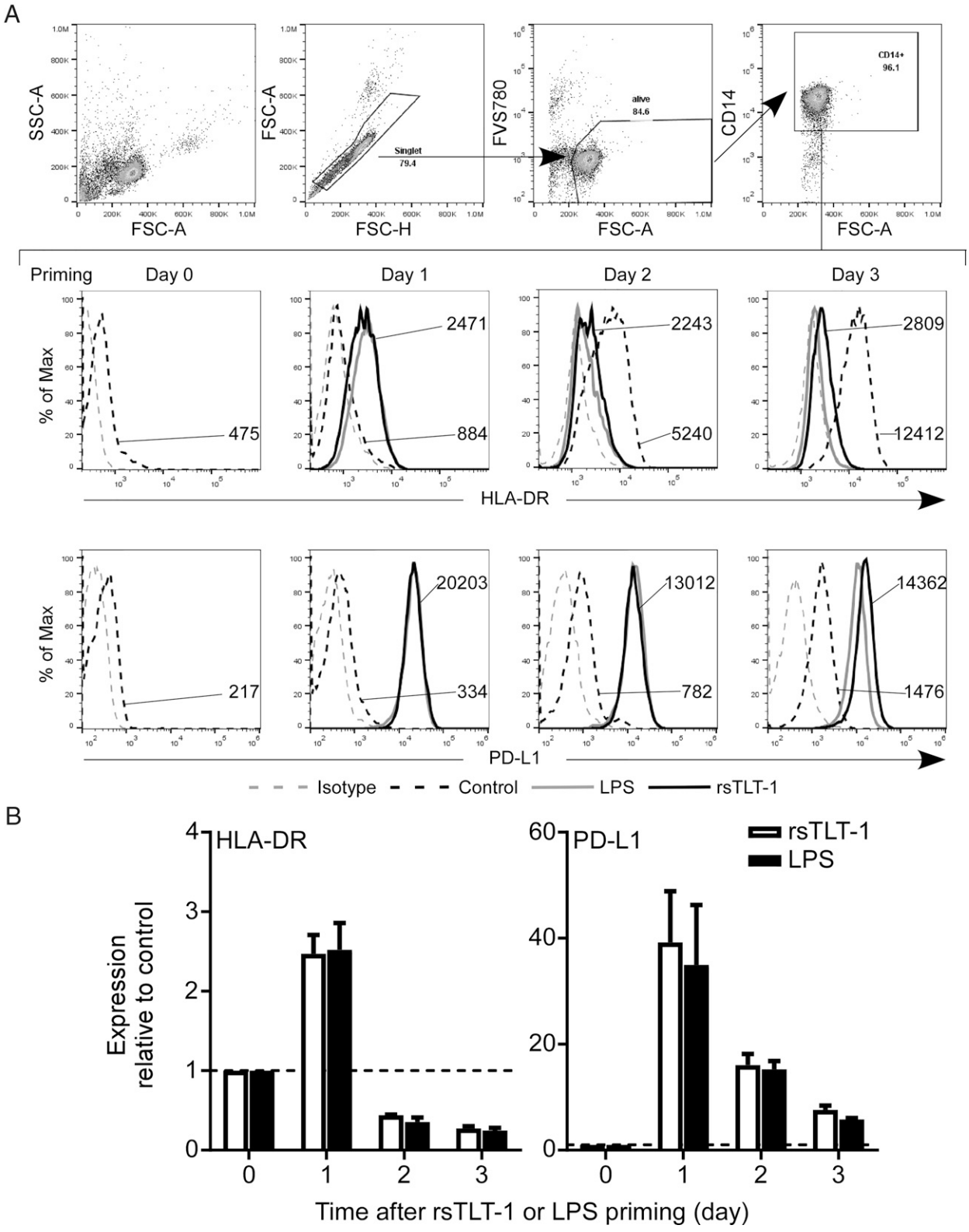

FIGURE 2. Effect of sTLT-1 on the surface expression of HLA-DR and PD-L1 molecules in monocytes. Monocytes were incubated with control (untreated), rsTLT-1 (10 μg/ml), or LPS (100 ng/ml) for 3 d. At the indicated time points, the cells were harvested, and the MFI of HLA-DR and PD-L1 were analyzed using flow cytometry. (**A**) Representative gating strategy was used to gate monocytes from live cells. Purified monocytes were gated out of all events, followed by subsequent $FVS780^{-}$ gating. Monocytes were identified as $CD14^{+}$ cells. A representative histogram of HLA-DR and PD-L1 expression on monocytes in various priming days is shown (heavy-line histogram, rsTLT-1–treated cells; dashed-line histogram, control cells; gray-line histogram, LPS-treated cells; gray dashed-line histogram, control cells stained with relative isotype control). Numbers represent MFI. (**B**) Expression patterns of rsTLT-1–primed or LPS-primed monocytes are presented relative to the expression patterns of monocytes with control treatment at the same time (50). Treatment with rsTLT-1 leads to a trend toward downregulation of HLA-DR expression. In contrast, rsTLT-1 priming upregulated the levels of PD-L1 expression on monocytes. Data are the sum of four independent experiments and are presented as the mean ± SEM.

were washed with PBS and restimulated with high amounts of LPS for an additional 18 h. As shown in Supplemental Fig. 1, TNF-α production upon LPS restimulation was significantly reduced in monocytes pretreated with rsTLT-1. Collectively, the results showed that rsTLT-1–exposed monocytes could enter a refractory state resembling hypoinflammation.

sTLT-1–induced activation in monocytes is similar to that by LPS

Because the pattern of sTLT-1–induced biphasic change of phenotypes in monocytes was similar to that induced by LPS, we next investigated whether sTLT-1 similarly affects monocyte function. Therefore, we first examined the effects of sTLT-1 on the phosphorylation events in the LPS-related signaling pathways in monocytes. As shown in Fig. 3a, both LPS and rsTLT-1 induced a rapid increase of IRF3 and p38 phosphorylation events within 120 min. Because the basal phosphorylation levels of IKKα and NF-κB were at 0 min, classically phosphorylated IKKα and NF-κB only showed a slight increase after incubation with LPS or rsTLT-1. However, NF-κB activity can be readily detected in the THP-1-XBlue-MD2-CD14 cells, a monocytic THP-1 cell line expressing NF-κB– and AP-1–inducible secreted embryonic alkaline phosphatase (SEAP) reporter gene, following incubation with LPS or rsTLT-1 (see Fig. 6).

We next analyzed the effect of sTLT-1 on the expression profiles of the proinflammatory cytokines IL-6 and TNF-α, as well as the anti-inflammatory cytokine IL-10. Incubation with rsTLT-1 induced rapid but transient expression of IL-6 and TNF-α mRNA. IL-6 mRNA expression peaked at ~4 h after the incubation of monocytes with rsTLT-1 (Fig. 3B, left). The maximal expression of TNF-α

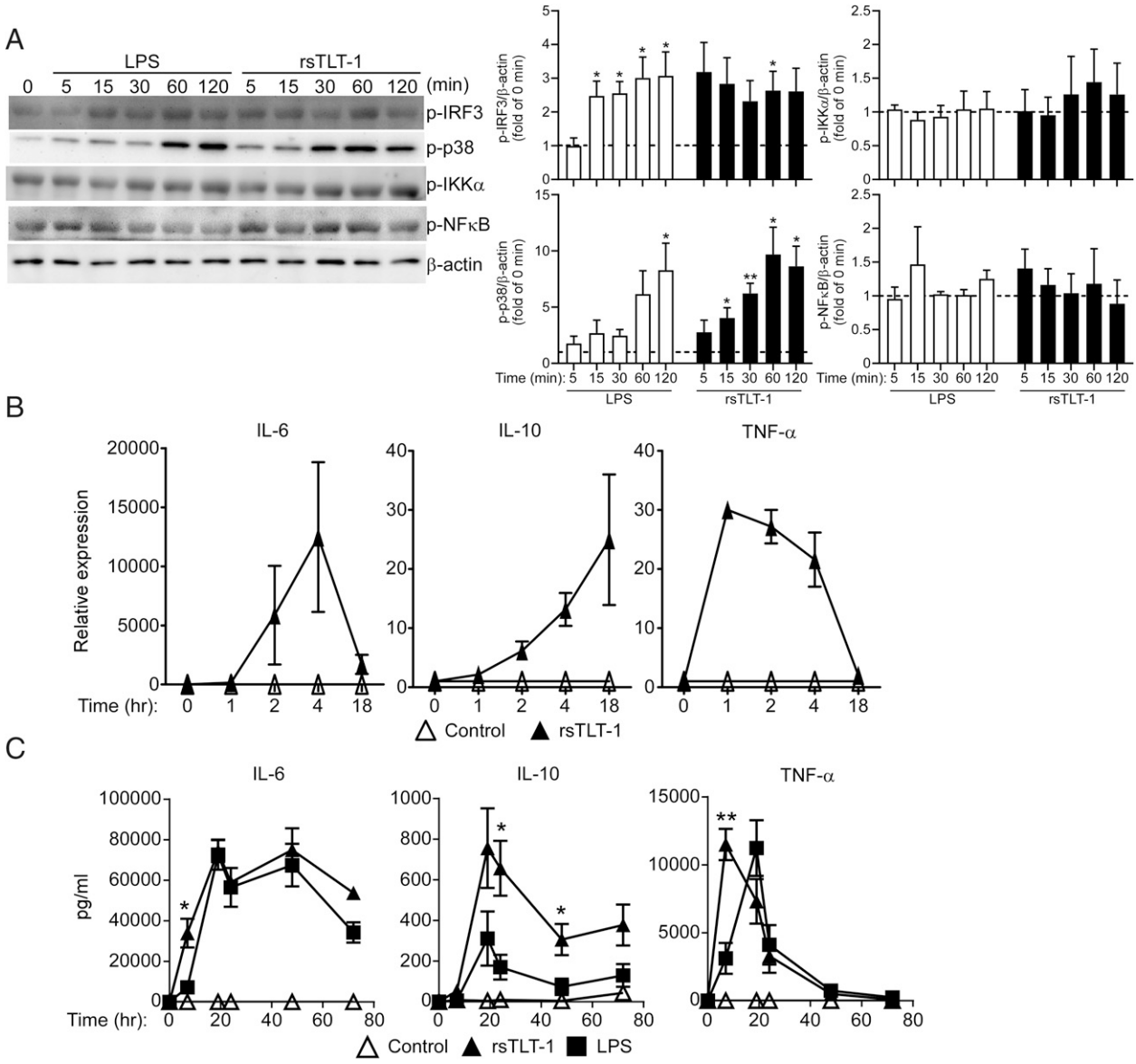

FIGURE 3. rsTLT-1 induces phosphorylation of events in the LPS-related signaling pathway and cytokine expression in monocytes. (**A**) Monocytes were stimulated with rsTLT-1 (10 μg/ml) or LPS (100 ng/ml) for the indicated times. The resulting cell lysates were resolved using SDS-PAGE and analyzed using Western blotting with specific Abs. β-Actin was used as a loading control. A representative result is shown. This experiment was conducted three times and results are presented as the mean ± SEM. $*p < 0.05$, $**p < 0.01$, versus 0 min control. (**B**) IL-6, IL-10, and TNF-α mRNA were analyzed using real-time RT-PCR. Binding of rsTLT-1 induced rapid but transient mRNA expression of the inflammatory cytokines IL-6 and TNF-α. Data are the sum of three independent experiments and are presented as the mean ± SEM. (**C**) Monocytes (2×10^5 cells) were stimulated with rsTLT-1 (10 μg/ml) or LPS (100 ng/ml) for the indicated times. IL-6, IL-10, and TNF-α were quantified using ELISA. Data are the sum of four independent experiments and are presented as the mean ± SEM. $*p < 0.05$, $**p < 0.01$, versus LPS-treated group.

mRNA was detected in monocytes after 1 h of incubation with rsTLT-1 (Fig. 3B, right). IL-6 and TNF-α mRNA expression subsequently decreased, returning to baseline levels ~18 h after incubation with rsTLT-1. In contrast, a slower but continual induction of IL-10 mRNA in monocytes was observed following incubation with rsTLT-1 (Fig. 3B, middle).

To further assess the effect of sTLT-1 on the production of these cytokines by human monocytes, the concentrations of IL-6, TNF-α, and IL-10 were measured by specific ELISA kits. For comparison, the same study was also conducted in human monocytes treated with LPS. As shown in Fig. 3C, rsTLT-1 could rapidly stimulate human monocytes to produce a large quantity of the proinflammatory cytokines IL-6 and TNF-α and the anti-inflammatory mediator IL-10. Interestingly, rsTLT-1 triggered a quick and robust induction of expression of the proinflammatory cytokines IL-6 and TNF-α 6 h after stimulation compared with LPS treatment, which induced profound cytokine secretion 18 h after stimulation (Fig. 3C). rsTLT-1 also induced a higher quantity of IL-10 release 24 h after stimulation than did LPS treatment. These results suggest that sTLT-1 may serve as an early mediator of inflammation.

To avoid possible LPS contamination, the rsTLT-1 used in this study was verified to contain <0.1 endotoxin unit/μg endotoxin (data not shown). In addition, the LPS inhibitor polymyxin B did not significantly reduce rsTLT-1–induced cytokine secretion (Supplemental Fig. 2). Therefore, the possibility that LPS contamination contributed to TLT-1–induced immune function can be ruled out.

sTLT-1 interacts with monocytes by binding to the cell surface receptors

To further study how sTLT-1 modulates monocyte function, we incubated human leukocytes with increasing concentrations of rsTLT-1 to assess whether rsTLT-1 could bind to the cell surface by

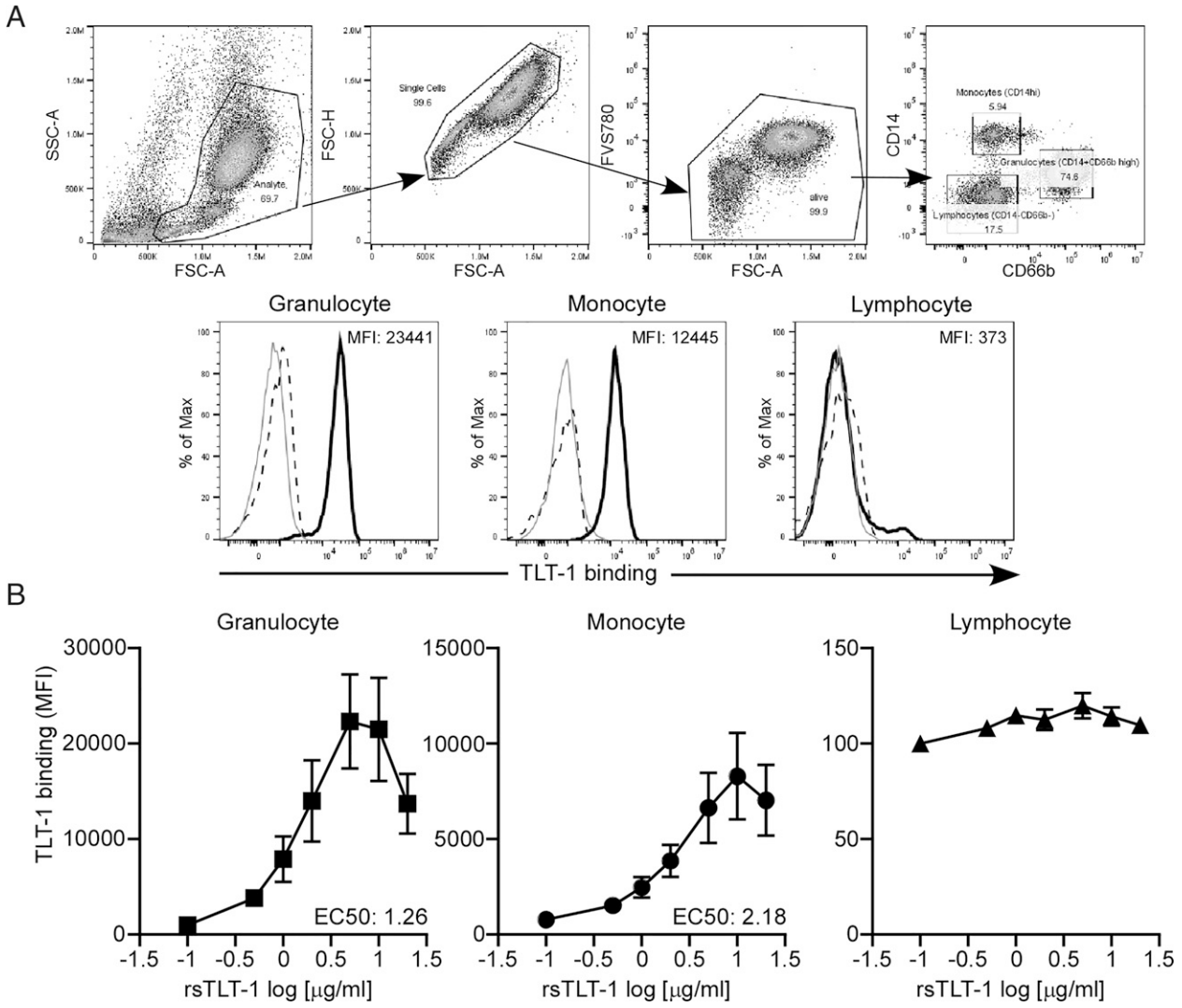

FIGURE 4. Interaction between rsTLT-1 and leukocytes. WBCs were incubated with rsTLT-1 for 1 h. Anti–TLT-1 Ab was added to detect the surface binding of TLT-1. (**A**) Representative gating strategy was used to gate granulocytes, monocytes, and lymphocytes from live cells. Live granulocytes, monocytes, and lymphocytes were gated out of all events based on their FSC/SSC properties, followed by subsequent FVS780$^-$ gating. Granulocytes were identified as CD14$^+$CD66b^{high} cells, monocytes were identified as CD14^{high}, and lymphocytes were then identified as CD14$^-$CD66b$^-$ cells. The anti–TLT-1 Ab was added to detect the surface binding of rsTLT-1. Representative TLT-1 binding histogram of various leukocytes in the presence or absence of rsTLT-1 treatment (heavy-line histogram, rsTLT-1 treated cells; gray-line histogram, untreated cells; thin dashed-line histogram, cell pools with/without rsTLT-1 treatment stained with isotype control). TLT-1 predominantly bound to granulocytes and monocytes but was less bound to lymphocytes. (**B**) Binding of various concentrations of rsTLT-1 to monocytes, granulocytes, and lymphocytes. Granulocytes and monocytes were able to bind rsTLT-1 in a dose-dependent manner. Data are the sum of four independent healthy subjects and are presented as the mean ± SEM.

using flow cytometry. The representative gating strategy is shown in Fig. 4A. rsTLT-1 was found to be associated with granulocytes and monocytes but not with lymphocytes (Fig. 4A). Dose-dependent binding of rsTLT-1 to granulocytes and monocytes was observed (Fig. 4B). TLT-1 binding affinity (EC_{50}) is 1.26 μg/ml in granulocytes and 2.18 μg/ml in monocytes, respectively. The binding of rsTLT-1 to granulocytes and monocytes was further studied by incubating human leukocytes with CF647-labeled rsTLT-1. The data further confirmed the association of CF647-labeled rsTLT-1 with granulocytes and monocytes (Supplemental Fig. 3). These results showed that sTLT-1 directly binds to undetermined surface receptors of granulocytes and monocytes, suggesting that intracellular signaling pathways are likely to exist, allowing sTLT-1 to modulate the functions of these cells.

The TLR4/MD2 complex is the receptor for sTLT-1

Because the profiles of the functional and signal responses of monocytes to sTLT-1 are notably similar to those induced by LPS, the interaction of rsTLT-1 with monocytes through TLR4 was speculated. We then performed docking analysis of sTLT-1 with TLR4 and MD2 proteins with the ZDOCK modeling program. Fig. 5A–C and Supplemental Video 1 illustrate the interaction mode of TLR4/MD2 and sTLT-1. The docking interactions suggested that the TLR4/MD2 complex binds to the extracellular domain of TLT-1 (Fig. 5A). Our modeling analysis suggests that TLR4 predominantly interacts with the IgV domain of TLT-1 (Fig. 5B). Regions of TLR4 (Glu^{286}–Tyr^{292}, Ser^{311}–Ile^{320}, Gly^{311}–Cys^{340}, Leu^{348}–Thr^{359}, Val^{370}–Arg^{382}, Gln^{423}–Asp^{428}, and Asn^{448}–Tyr^{451}) formed a strong binding network with TLT-1 (Gln^{16}–Val^{25}, Leu^{35}–Val^{50}, Val^{67}–Arg^{70}, Leu^{79}–Gln^{88}, and Cys^{104}–Arg^{117}). In addition, parts of MD2 (Lys^{91}–Asp^{101} and Gln^{73}–Tyr^{79}) interacted with the other IgV domain of TLT-1 (Ser^{21}–Ser^{32} and Leu^{94}–Glu^{101}). The other parts of MD2 (Ala^{137}–Met^{145} and Cys^{37}–Met^{40}) strongly bind to the N-terminal region of the stalk in TLT-1 from Arg^{117} to Glu^{130} (Fig. 5C). A solid-phase binding study confirmed that rsTLT-1 binds both MD2 and TLR4 in a concentration-dependent manner (Fig. 5D).

To examine whether sTLT-1 activates monocytes through the TLR4/MD2 pathway, we used THP-1-XBlue-MD2-CD14 cells as a reporter cell line. Although Western blot only showed that phosphorylated NF-κB slightly increased 5 min after incubation with rsTLT-1 in monocytes (Fig. 3A), NF-κB activity can be readily detected in the THP-1-XBlue-MD2-CD14 cells 18 h after incubation with LPS or rsTLT-1 (Fig. 6). Treatment with anti-TLR4 or anti-MD2 blocking Abs significantly reduced the levels of NF-κB activity and TNF-α secretion. Taken together, these results suggested that sTLT-1 activated monocytes via TLR4/MD2 signaling.

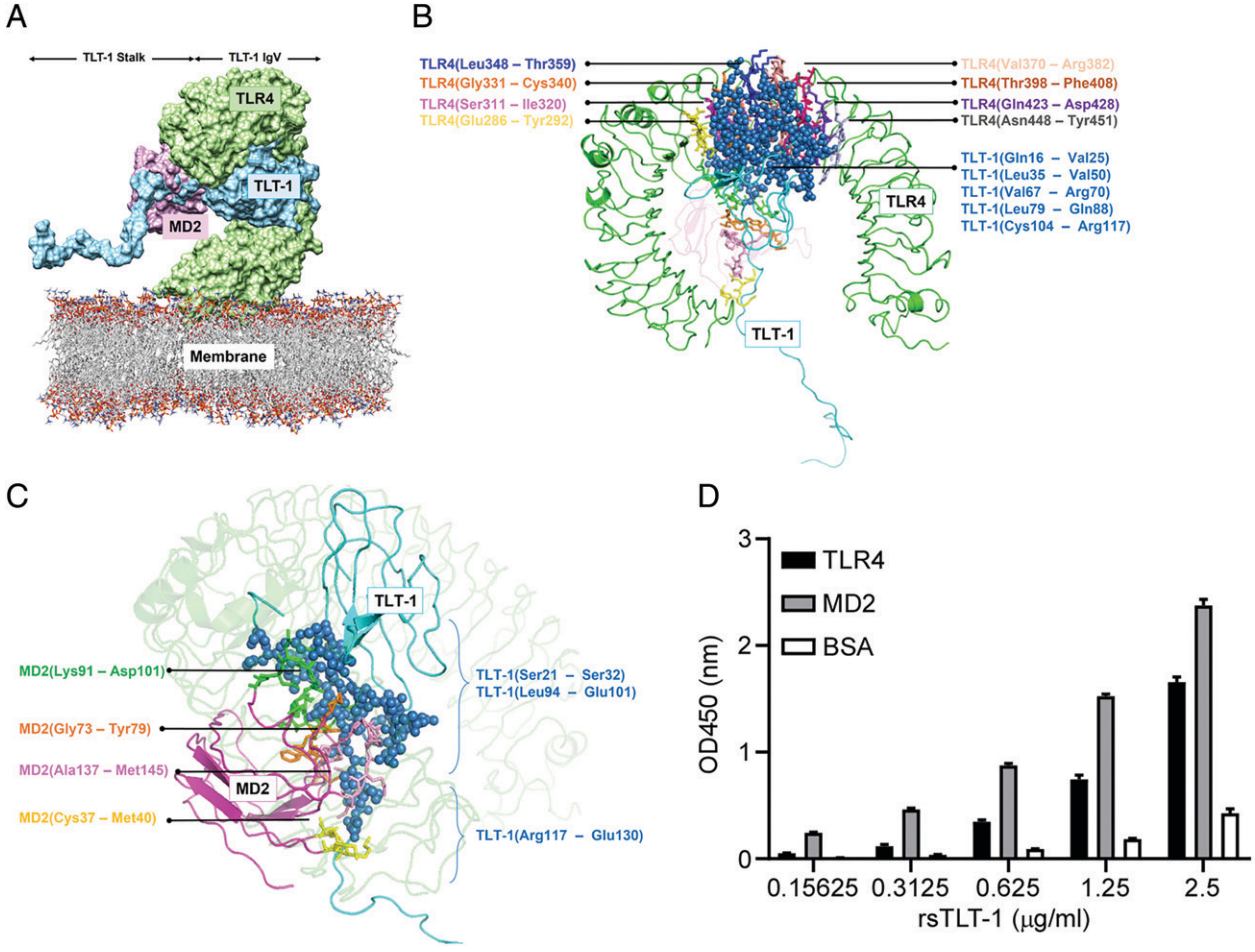

FIGURE 5. sTLT-1 binds to MD2 and TLR4. (**A**) Highest docking result of TLT-1 with the TLR4 and MD2 proteins. (**B**) Computer modeling analysis for the binding interaction of TLR4 and TLT-1. In TLR4, the interacting regions are shown in yellow, magenta, orange, blue, olive, brown, purple, and gray. The binding parts of TLT-1 are sky blue in color and spherical. (**C**) Computer modeling analysis for the binding interaction of MD2 and TLT-1. The binding regions of MD2 are shown in green, orange, magenta, and yellow. The binding parts of TLT-1 are sky blue in color and spherical. (**D**) Microtiter plates were coated separately with recombinant 5 μg/ml TLR4, MD2, or BSA (negative control). The plates were incubated with different concentrations of rsTLT-1 and secondary Ab-HRP for 2 h and 30 min, respectively. rsTLT-1 was able to bind TLR4 and MD2 in a dose-dependent manner. The results represent the means ± SEM of triplicate experiments.

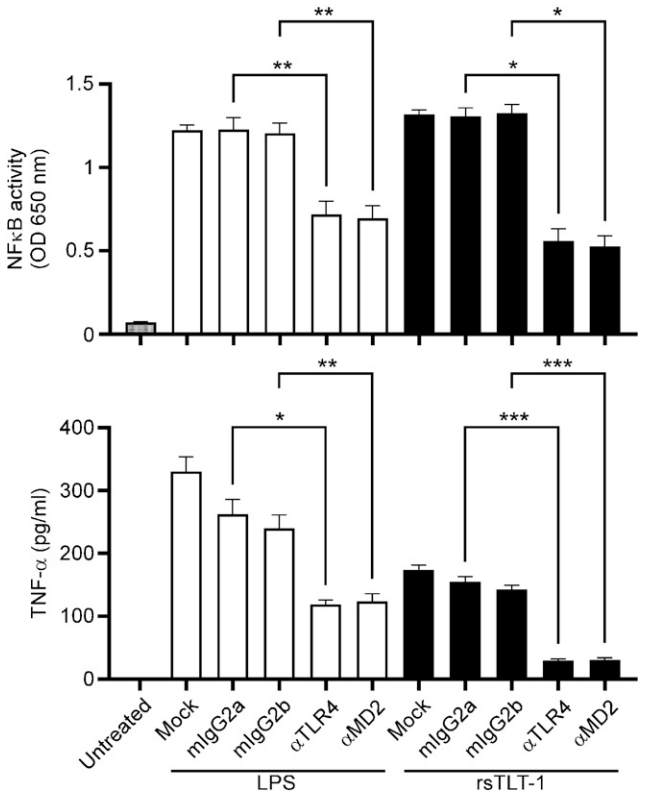

FIGURE 6. Anti-TLR4 and MD2 Ab treatment reduces sTLT-1–induced activation in THP-1-XBlue-MD2-CD14 cells. THP-1-XBlue-MD2-CD14 cells were pretreated with anti-TLR4 Ab (10 μg/ml), anti-MD2 Ab (1 μg/ml), mouse IgG2a isotype control (10 μg/ml, MOPC173), or mouse IgG2b isotype control (1 μg/ml, MPC-11) for 15 min. The cells were then treated with LPS (100 ng/ml) or rsTLT-1 (10 μg/ml) and incubated for 18 h. NF-κB activity and TNF-α secretion were measured with QUANTI-Blue (up) and ELISA (down). The results represent the means ± SEM of triplicate experiments. $^{*}p < 0.05$. $^{**}p < 0.01$, $^{***}p < 0.001$.

Anti–TLT-1 Ab (clone 26A6) reduced TNF-α release and mortality in an animal model of sepsis

It has been reported that sTLT-1 can be detected in the blood of animals treated with bacterial LPS (17). It appeared that sTLT-1 may not only be an early biomarker of sepsis but also contributes to immune dysfunction other than endotoxin-associated pathophysiology. To examine this hypothesis, we generated an anti–TLT-1 Ab (clone 26A6) capable of binding to both hTLT-1 and mTLT-1 (see Fig. 8A). Our results showed that 26A6 could reduce approximately one-third of rsTLT-1 binding to granulocytes and monocytes (Fig. 7A). As shown in Fig. 7B, monocytes treated with 26A6 also reduced sTLT-1–induced IL-6, IL-10, and TNF-α release. We next assessed whether blocking sTLT-1 altered LPS-induced TNF-α secretion in the murine sepsis model. The results showed that both pretreatment and posttreatment with the 26A6 significantly reduced the LPS-induced secretion of TNF-α in the plasma (Fig. 8B).

To assess whether the 26A6 could also provide a survival benefit to the sepsis animal model, we tested the 26A6 in BALB/c mice receiving lethal i.p. doses of LPS. Fig. 8C shows a favorable trend of survival benefit in the 26A6-pretreated group, but this effect became less favorable in mice posttreated with 26A6. The survival rate for the first 48 h in vehicle-treated, 26A6-posttreated, and 26A6-pretreated groups were 70, 80, and 90%, respectively. The survival rate for 72 h in vehicle-treated, 26A6-posttreated, and 26A6-pretreated groups were 30, 50, and 60%, respectively. Only 30% of vehicle-treated mice survived at the end of the study, but 60% of 26A6-pretreated and 40% of 26A6-posttreated mice can survive beyond 120 h. No late deaths were observed after 120 h for the surviving mice. Although both 26A6 pretreatment and posttreatment significantly reduced plasma TNF-α concentration in the mice with LPS inoculation (Fig. 8B), organ damage could have been established 2 h after the lethal LPS challenge. In addition, because the 26A6 Ab does not fully compete sTLT-1 binding to myeloid cells (Fig. 7A), this 26A6 might not be the most suitable Ab for blocking TLT-1–induced function. Therefore, posttreatment with 26A6 may be less effective in improving overall survival. Taken together, these results suggest that the elevation of circulating sTLT-1 levels by LPS may augment the detrimental effects during sepsis. The anti–TLT-1 Ab treatment could potentially provide a novel therapeutic method for treating sepsis.

Discussion

Gram-negative bacterial infections are typically observed in patients with sepsis. Human endotoxemia induced by LPS causes hyperinflammatory and hypoinflammatory responses both in vitro and in vivo. In addition, endotoxin is commonly used as a standard model to study sepsis-induced immunosuppression (24–28). Although the presence of endotoxin tolerance is critical for the pathophysiology underlying sepsis-induced immunoparalysis, LPS may not be the only factor that can cause this phenomenon. A variety of other endogenous damage-associated molecular patterns or alarmins, such as HMGB1 or S100A12 expressed during sepsis or sterile inflammation, can activate pattern recognition receptors to initiate immune activation and sustained dysfunction and, therefore, may be considered potential triggers of immunosuppression (29–35). Our results suggest that platelet-derived sTLT-1 is an essential factor that contributes to immune dysregulation in sepsis. The in vitro data showed that recombinant soluble TLT-1 was able to induce phenotypes with immune activation followed with subsequent immunosuppression in human monocytes (Fig. 2). The immune analysis from clinical samples was also in accord with the in vitro data showing that the plasma concentrations of sTLT-1 were correlated with the benchmarks of immunosuppressive phenotypes, that is, reduced HLA-DR levels with increased PD-L1 expression in monocytes from patients with septic shock (Fig. 1). These data indicate that sTLT-1 may play a distinctive role by interacting with monocytes to modulate the immune response during the development and progression of sepsis. Monocytes are a type of APCs that initiate a T cell response through MHC class II molecules such as HLA-DR and other costimulatory molecules such as CD86 on their cell surfaces. The production of proinflammatory cytokines, the secondary signals, is required to further amplify T cell responses. However, in the late phase of sepsis, continuous downregulation of the proinflammatory response renders the patient's immune system incapable of fighting secondary infections. Our current study provides evidence that sTLT-1 can induce an extended period of immune tolerance in terms of TNF-α production to a subsequent LPS challenge (Supplemental Fig. 1). Therefore, our data demonstrate, to our knowledge, for the first time, that the production of cytokines by monocytes in response to pathogens could be inhibited in the presence of sTLT-1. Consequently, monocytes with immunosuppressive changes from patients with septic shock could not support T cell activation not only because of reduced immune synaptic function but also because of suppression of secondary signals by cytokines. Monocytes with impaired major functions have also been reported as a determining factor for subsequent secondary infections and mortality in patients with sepsis (36). Our findings suggest that the presence of sTLT-1 may activate and subsequently drive monocytes toward an impaired functional status,

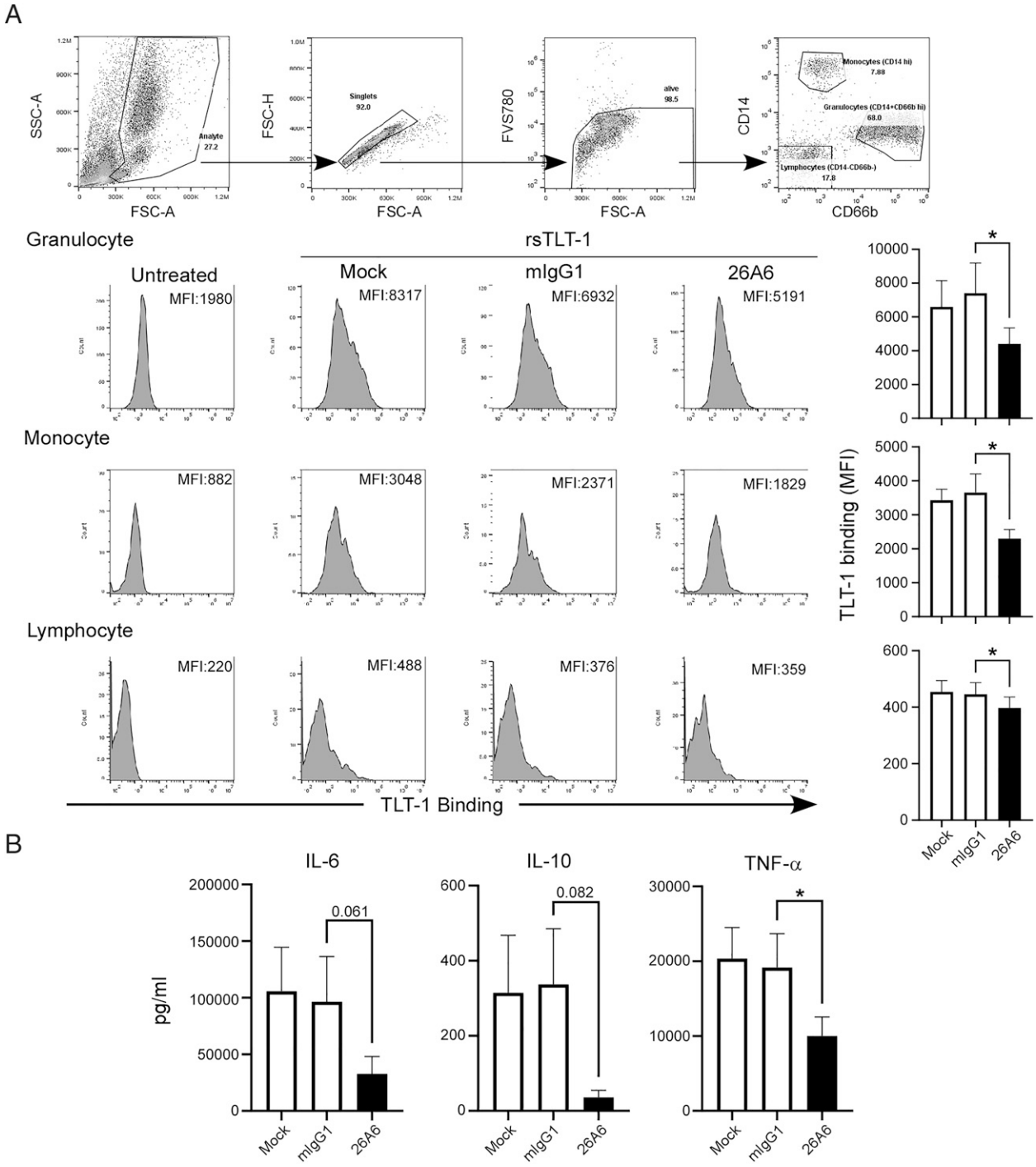

FIGURE 7. Anti–TLT-1 Ab (26A6) treatment can block rsTLT-1 binding to myeloid immune cells and reduce rsTLT-1–induced monocytic activation. (**A**) WBCs were pretreated with anti–TLT-1 Ab (10 μg/ml, 26A6) or mouse IgG1 isotype control (10 μg/ml, MOPC21) and then incubated with rsTLT-1 (10 μg/ml) for 1 h. The anti-His tag Ab was added to detect the surface binding of rsTLT-1, which was analyzed by flow cytometry. A representative gating strategy was used to gate granulocytes, monocytes, and lymphocytes from live cells. Live granulocytes, monocytes, and lymphocytes were gated out of all events based on their FSC/SSC properties, followed by subsequent FVS780$^-$ gating. Granulocytes were identified as CD14$^+$CD66b^{high} cells, monocytes were identified as CD14^{high}, and lymphocytes were then identified as CD14$^-$CD66b$^-$ cells. Representative TLT-1 binding histogram of various leukocytes in the presence or absence of anti–TLT-1 Ab (26A6) treatment. Data are the sum of four independent samples from healthy subjects and are presented as the mean ± SEM. *$p < 0.05$. (**B**) Monocytes were pretreated with anti–TLT-1 Ab (10 μg/ml, 26A6) or mouse IgG1 isotype control (10 μg/ml, MOPC21) and then incubated with rsTLT-1 (10 μg/ml) for 18 h. The supernatant of the culture medium was collected, and IL-6, IL-10, and TNF-α secretion was measured by cytokine ELISA. Data are the sum of three independent samples from healthy subjects and are presented as the mean ± SEM. *$p < 0.05$.

in addition to infection assaults, through the downregulation of HLA-DR expression, upregulation of PD-L1 expression, and a decrease in proinflammatory cytokine production. Thus, sTLT-1 affects the normal crosstalk between innate and adaptive immunity, leading to a failure to establish optimal pathogen-specific immunity.

sTLT-1 was found to be able to bind human monocytes (Fig. 4) and induce the activation of LPS-related signaling pathways with increased secretion of TNF-α, IL-6, and IL-10 (Fig. 3). Based on these data, we predicted that there could be receptors on monocytes for sTLT-1 that are functionally similar to those involved in TLR

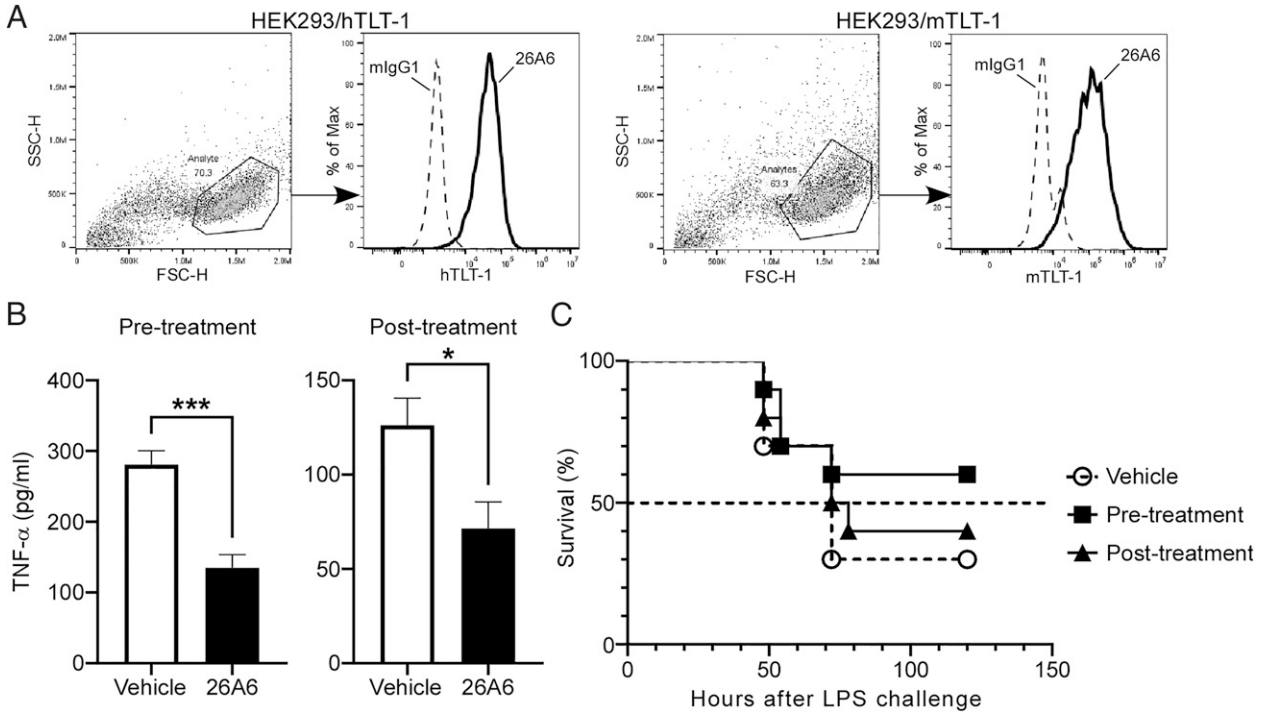

FIGURE 8. Effects of i.p. administered anti–TLT-1 Ab (26A6) on TNF-α production in a mouse model of endotoxemia and protection against LPS lethality in mice. (**A**) Anti–TLT-1 Ab (26A6) binds to human HEK293/hTLT-1 and HEK293/mTLT-1 cells. Flow cytometry analysis of anti–TLT-1 Ab binding to human TLT-1–expressing cells (left) and mouse TLT-1–expressing cells (right). The cells were incubated with 10 μg/ml anti–TLT-1 Ab (26A6) or 10 μg/ml mouse IgG1 isotype control (MOPC21) for 30 min at 37°C and 5% CO_2. Incubation with the secondary Ab (allophycocyanin anti-mouse IgG) was carried out for 30 min at 4°C. Heavy-line histogram, anti–TLT-1 Ab-treated cells; dashed-line histogram, IgG control-treated cells. (**B**) BALB/c mice (n = 5/group) were i.p. injected with an anti–TLT-1 Ab (5 mg/kg, 26A6) or vehicle (saline) 1 h before or 2 h after LPS injection (5 mg/kg). Production of TNF-α in peripheral blood plasma at 4 h after injection of LPS. *$p < 0.05$, ***$p < 0.001$. (**C**) In survival experiments, BALB/c mice (n = 10/group) were i.p. injected with a lethal dose of LPS (15 mg/kg) 1 h before or 2 h after LPS injection, mice were injected i.p. with an anti–TLT-1 Ab (20 mg/kg, 26A6). For the vehicle control group, mice were injected i.p. with saline 1 h before LPS injection. Survival was monitored every 8–12 h.

ligand–induced activation. Our docking simulation indeed indicated that the extracellular domain of TLT-1 binds the TLR4/MD2 complex (Fig. 5A). The IgV domain of TLT-1 is the main domain responsible for TLR4 and MD2 binding (Fig. 5B). In addition, the stalk region of TLT-1 is predicted to participate in MD2 interaction (Fig. 5C). The interaction of different parts of sTLT-1 with the TLR4/MD2 complex was later confirmed by using a solid-phase binding study showing that rsTLT-1 binds both MD2 and TLR4 in a concentration-dependent manner (Fig. 5D). In addition, functional blocking Abs against TLR4 and MD2 reduced sTLT-1–induced signaling and cytokine production (Fig. 6). Blocking sTLT-1 and monocyte interactions with an anti–TLT-1 Ab significantly reduced sTLT-1–induced cytokine production (Fig. 7). Taken together, our results clearly demonstrate that sTLT-1 interacts with the TLR4/MD2 complex, leading to the production of proinflammatory cytokines through TLR signaling pathways. However, the anti–TLT-1 Ab did not completely prevent the binding of TLT-1 to monocytes (Fig. 7); therefore, it cannot be ruled out that other receptors may exist. In fact, our preliminary results showed that sTLT-1 also enhanced NF-κB activity in the HEK-Blue hTLR2 cell line, suggesting that TLR2 may be another receptor of sTLT-1 (Supplemental Fig. 4). Other studies have suggested that sTLT-1 may interact with FcγR1 (37), soluble TREM-1 ligand (18), and CD3ε (38), although more studies are required to establish such relationships. There are some possible mechanisms that may explain how activating the TLR4/MD2 pathway by sTLT-1 induces immunosuppression. Our data show that sTLT-1 can induce sustained IL-10 expression and secretion from monocytes. IL-10 has been reported to diminish HLA-DR expression on monocytes in septic shock (39). Another possibility involves the induction of STAT3 through TLR4 signaling. STAT3 is a negative regulator of cytokine production (40, 41) and mediates MHC class II and PD-L1 expression in APCs (42, 43). It is also likely that sTLT-1 activates integrin CD11b/CD18 via TLR4-associated inside-out signaling and that high-avidity ligand binding of CD11b leads to subsequent inhibition of TLR signaling (44). Therefore, although sTLT-1, similar to LPS, binds to TLR4/MD2, several possible subsequent negative feedback pathways decrease the immune response. Recent reports support our finding that sTLT-1–induced immunosuppression could be a common pathway that is seen not only in sepsis (38, 45). Nevertheless, the detailed molecular mechanisms responsible for dysregulation of the TLT-1–induced immune response and clinical implications are still under investigation.

Sepsis is defined as "life-threatening organ dysfunction caused by a dysregulated host response to infection" (19). Among these abnormal host responses, immune dysregulation and excessive coagulopathy mediated by platelets have often been regarded as druggable targets. However, treatments with immune and coagulation modulators showed little or no benefits in patients with sepsis (46–48). In this study, we show that sTLT-1 secreted by activated platelets induces immune dysregulation in sepsis and provides evidence that a blocking TLT-1 Ab can reduce TNF-α secretion and prolong survival time in animals with sepsis (Fig. 8). Another study also showed that blocking TLT-1 with a single-chain variable fragment Ab inhibits thrombin-induced platelet aggregation (49). These studies provide a feasible strategy for the simultaneous treatment of immune dysregulation and coagulopathy during sepsis by targeting sTLT-1. In conclusion, we report the mechanisms by which sTLT-1

mediates the immunophenotype of monocytes, a state frequently observed in patients during sepsis, trauma, surgery, and cancer. Our findings provide opportunities to develop further research exploring possible therapies for the interaction between sTLT-1 and its receptor in reversing sepsis-induced immune dysregulation.

Disclosures

C.-M.C., M.-P.L., and Y.-C.C. are staff members of Ascendo Biotechnology, Inc. Y.-T.L. is an adjunct senior attending physician at MacKay Memorial Hospital and joined Ascendo Biotechnology, Inc. in 2021. The 26A6 anti–TLT-1 Ab used to obtain data shown in Figs. 7 and 8 is covered under a patent application by Ascendo Biotechnology, Inc. C.-M.C., Y.-C.C., and Y.-T.L. are inventors on that patent. The other authors have no financial conflicts of interest.

References

1. Kaukonen, K. M., M. Bailey, D. Pilcher, D. J. Cooper, and R. Bellomo. 2015. Systemic inflammatory response syndrome criteria in defining severe sepsis. *N. Engl. J. Med.* 372: 1629–1638.
2. Hotchkiss, R. S., and S. Opal. 2010. Immunotherapy for sepsis—a new approach against an ancient foe. *N. Engl. J. Med.* 363: 87–89.
3. Le Tulzo, Y., C. Pangault, A. Gacouin, V. Guilloux, O. Tribut, L. Amiot, P. Tattevin, R. Thomas, R. Fauchet, and B. Drénou. 2002. Early circulating lymphocyte apoptosis in human septic shock is associated with poor outcome. *Shock* 18: 487–494.
4. Monneret, G., A. Lepape, and F. Venet. 2011. A dynamic view of mHLA-DR expression in management of severe septic patients. *Crit. Care* 15: 198.
5. van Vught, L. A., M. A. Wiewel, A. J. Hoogendijk, J. F. Frencken, B. P. Scicluna, P. M. C. Klein Klouwenberg, A. H. Zwinderman, R. Lutter, J. Horn, M. J. Schultz, et al. 2017. The host response in patients with sepsis developing intensive care unit-acquired secondary infections. *Am. J. Respir. Crit. Care Med.* 196: 458–470.
6. Boomer, J. S., K. To, K. C. Chang, O. Takasu, D. F. Osborne, A. H. Walton, T. L. Bricker, S. D. Jarman II, D. Kreisel, A. S. Krupnick, et al. 2011. Immunosuppression in patients who die of sepsis and multiple organ failure. *JAMA* 306: 2594–2605.
7. Hotchkiss, R. S., K. W. Tinsley, P. E. Swanson, R. E. Schmieg, Jr., J. J. Hui, K. C. Chang, D. F. Osborne, B. D. Freeman, J. P. Cobb, T. G. Buchman, and I. E. Karl. 2001. Sepsis-induced apoptosis causes progressive profound depletion of B and $CD4^+$ T lymphocytes in humans. *J. Immunol.* 166: 6952–6963.
8. Muenzer, J. T., C. G. Davis, K. Chang, R. E. Schmidt, W. M. Dunne, C. M. Coopersmith, and R. S. Hotchkiss. 2010. Characterization and modulation of the immunosuppressive phase of sepsis. *Infect. Immun.* 78: 1582–1592.
9. Lukaszewicz, A. C., M. Grienay, M. Resche-Rigon, R. Pirracchio, V. Faivre, B. Boval, and D. Payen. 2009. Monocytic HLA-DR expression in intensive care patients: interest for prognosis and secondary infection prediction. *Crit. Care Med.* 37: 2746–2752.
10. Monneret, G., A. Lepape, N. Voirin, J. Bohé, F. Venet, A. L. Debard, H. Thizy, J. Bienvenu, F. Gueyffier, and P. Vanhems. 2006. Persisting low monocyte human leukocyte antigen-DR expression predicts mortality in septic shock. *Intensive Care Med.* 32: 1175–1183.
11. Shao, R., Y. Fang, H. Yu, L. Zhao, Z. Jiang, and C. S. Li. 2016. Monocyte programmed death ligand-1 expression after 3–4 days of sepsis is associated with risk stratification and mortality in septic patients: a prospective cohort study. *Crit. Care* 20: 124.
12. Zhang, Y., J. Li, J. Lou, Y. Zhou, L. Bo, J. Zhu, K. Zhu, X. Wan, Z. Cai, and X. Deng. 2011. Upregulation of programmed death-1 on T cells and programmed death ligand-1 on monocytes in septic shock patients. *Crit. Care* 15: R70.
13. Marcoux, G., A. Laroche, J. Espinoza Romero, and E. Boilard. 2021. Role of platelets and megakaryocytes in adaptive immunity. *Platelets* 32: 340–351.
14. Dib, P. R. B., A. C. Quirino-Teixeira, L. B. Merij, M. B. M. Pinheiro, S. V. Rozini, F. B. Andrade, and E. D. Hottz. 2020. Innate immune receptors in platelets and platelet-leukocyte interactions. *J. Leukoc. Biol.* 108: 1157–1182.
15. Kerris, E. W. J., C. Hoptay, T. Calderon, and R. J. Freishtat. 2020. Platelets and platelet extracellular vesicles in hemostasis and sepsis. *J. Investig. Med.* 68: 813–820.
16. Branfield, S., and A. V. Washington. 2021. The enigmatic nature of the triggering receptor expressed in myeloid cells -1 (TLT- 1). *Platelets* 32: 753–760.
17. Washington, A. V., S. Gibot, I. Acevedo, J. Gattis, L. Quigley, R. Feltz, A. De La Mota, R. L. Schubert, J. Gomez-Rodriguez, J. Cheng, et al. 2009. TREM-like transcript-1 protects against inflammation-associated hemorrhage by facilitating platelet aggregation in mice and humans. *J. Clin. Invest.* 119: 1489–1501.
18. Derive, M., Y. Bouazza, N. Sennoun, S. Marchionni, L. Quigley, V. Washington, F. Massin, J. P. Max, J. Ford, C. Alauzet, et al. 2012. Soluble TREM-like transcript-1 regulates leukocyte activation and controls microbial sepsis. *J. Immunol.* 188: 5585–5592.
19. Singer, M., C. S. Deutschman, C. W. Seymour, M. Shankar-Hari, D. Annane, M. Bauer, R. Bellomo, G. R. Bernard, J. D. Chiche, C. M. Coopersmith, et al. 2016. The Third International Consensus Definitions for Sepsis and Septic Shock (Sepsis-3). *JAMA* 315: 801–810.
20. Pierce, B. G., K. Wiehe, H. Hwang, B. H. Kim, T. Vreven, and Z. Weng. 2014. ZDOCK server: interactive docking prediction of protein-protein complexes and symmetric multimers. *Bioinformatics* 30: 1771–1773.
21. Gattis, J. L., A. V. Washington, M. M. Chisholm, L. Quigley, A. Szyk, D. W. McVicar, and J. Lubkowski. 2006. The structure of the extracellular domain of triggering receptor expressed on myeloid cells like transcript-1 and evidence for a naturally occurring soluble fragment. *J. Biol. Chem.* 281: 13396–13403.
22. Park, B. S., D. H. Song, H. M. Kim, B. S. Choi, H. Lee, and J. O. Lee. 2009. The structural basis of lipopolysaccharide recognition by the TLR4-MD-2 complex. *Nature* 458: 1191–1195.
23. Lu, Y. T., C. Y. Yen, H. C. Ho, C. J. Chen, M. F. Wu, and S. L. Hsieh. 2006. Preparation and characterization of monoclonal antibody against protein TREM-like transcript-1 (TLT-1). *Hybridoma (Larchmt.)* 25: 20–26.
24. Cavaillon, J. M., and M. Adib-Conquy. 2006. Bench-to-bedside review: endotoxin tolerance as a model of leukocyte reprogramming in sepsis. *Crit. Care* 10: 233.
25. Biswas, S. K., P. Bist, M. K. Dhillon, T. Kajiji, C. Del Fresno, M. Yamamoto, E. Lopez-Collazo, S. Akira, and V. Tergaonkar. 2007. Role for MyD88-independent, TRIF pathway in lipid A/TLR4-induced endotoxin tolerance. *J. Immunol.* 179: 4083–4092.
26. Biswas, S. K., and E. Lopez-Collazo. 2009. Endotoxin tolerance: new mechanisms, molecules and clinical significance. *Trends Immunol.* 30: 475–487.
27. del Fresno, C., F. García-Rio, V. Gómez-Piña, A. Soares-Schanoski, I. Fernández-Ruíz, T. Jurado, T. Kajiji, C. Shu, E. Marín, A. Gutierrez del Arroyo, et al. 2009. Potent phagocytic activity with impaired antigen presentation identifying lipopolysaccharide-tolerant human monocytes: demonstration in isolated monocytes from cystic fibrosis patients. [Published erratum appears in 2009 *J. Immunol.* 183: 2194.] *J. Immunol.* 182: 6494–6507.
28. Foster, S. L., D. C. Hargreaves, and R. Medzhitov. 2007. Gene-specific control of inflammation by TLR-induced chromatin modifications. [Published erratum appears in 2008 *Nature* 451: 102.] *Nature* 447: 972–978.
29. Li, L., and Y. Q. Lu. 2021. The regulatory role of high-mobility group protein 1 in sepsis-related immunity. *Front. Immunol.* 11: 601815.
30. Huang, W., Y. Tang, and L. Li. 2010. HMGB1, a potent proinflammatory cytokine in sepsis. *Cytokine* 51: 119–126.
31. Erridge, C. 2010. Endogenous ligands of TLR2 and TLR4: agonists or assistants? *J. Leukoc. Biol.* 87: 989–999.
32. Quintana, F. J., and I. R. Cohen. 2005. Heat shock proteins as endogenous adjuvants in sterile and septic inflammation. *J. Immunol.* 175: 2777–2782.
33. van der Poll, T., F. L. van de Veerdonk, B. P. Scicluna, and M. G. Netea. 2017. The immunopathology of sepsis and potential therapeutic targets. *Nat. Rev. Immunol.* 17: 407–420.
34. Deutschman, C. S., and K. J. Tracey. 2014. Sepsis: current dogma and new perspectives. *Immunity* 40: 463–475.
35. Foell, D., H. Wittkowski, C. Kessel, A. Lüken, T. Weinhage, G. Varga, T. Vogl, T. Wirth, D. Viemann, P. Björk, et al. 2013. Proinflammatory S100A12 can activate human monocytes via Toll-like receptor 4. *Am. J. Respir. Crit. Care Med.* 187: 1324–1334.
36. van der Poll, T., M. Shankar-Hari, and W. J. Wiersinga. 2021. The immunology of sepsis. *Immunity* 54: 2450–2464.
37. Das, A. A., D. Chakravarty, D. Bhunia, S. Ghosh, P. C. Mandal, K. N. Siddiqui, and A. Bandyopadhyay. 2019. Elevated level of circulatory sTLT1 induces inflammation through SYK/MEK/ERK signalling in coronary artery disease. *Clin. Sci. (Lond.)* 133: 2283–2299.
38. Tyagi, T., K. Jain, T. O. Yarovinsky, M. Chiorazzi, J. Du, C. Castro, J. Griffin, A. Korde, K. A. Martin, S. S. Takyar, et al. 2023. Platelet-derived TLT-1 promotes tumor progression by suppressing $CD8^+$ T cells. *J. Exp. Med.* 220: e20212218.
39. Fumeaux, T., and J. Pugin. 2002. Role of interleukin-10 in the intracellular sequestration of human leukocyte antigen-DR in monocytes during septic shock. *Am. J. Respir. Crit. Care Med.* 166: 1475–1482.
40. Niemand, C., A. Nimmesgern, S. Haan, P. Fischer, F. Schaper, R. Rossaint, P. C. Heinrich, and G. Müller-Newen. 2003. Activation of STAT3 by IL-6 and IL-10 in primary human macrophages is differentially modulated by suppressor of cytokine signaling 3. *J. Immunol.* 170: 3263–3272.
41. Murray, P. J. 2007. The JAK-STAT signaling pathway: input and output integration. *J. Immunol.* 178: 2623–2629.
42. Kitamura, H., H. Kamon, S. Sawa, S. J. Park, N. Katunuma, K. Ishihara, M. Murakami, and T. Hirano. 2005. IL-6-STAT3 controls intracellular MHC class II αβ dimer level through cathepsin S activity in dendritic cells. *Immunity* 23: 491–502.
43. Wölfle, S. J., J. Strebovsky, H. Bartz, A. Sähr, C. Arnold, C. Kaiser, A. H. Dalpke, and K. Heeg. 2011. PD-L1 expression on tolerogenic APCs is controlled by STAT-3. *Eur. J. Immunol.* 41: 413–424.
44. Han, C., J. Jin, S. Xu, H. Liu, N. Li, and X. Cao. 2010. Integrin CD11b negatively regulates TLR-triggered inflammatory responses by activating Syk and promoting degradation of MyD88 and TRIF via Cbl-b. *Nat. Immunol.* 11: 734–742.
45. Mirouse, A., C. Vigneron, J. F. Llitjos, J. D. Chiche, J. P. Mira, D. Mokart, E. Azoulay, and F. Pène. 2020. Sepsis and cancer: an interplay of friends and foes. *Am. J. Respir. Crit. Care Med.* 202: 1625–1635.
46. Nakamori, Y., E. J. Park, and M. Shimaoka. 2021. Immune deregulation in sepsis and septic shock: reversing immune paralysis by targeting PD-1/PD-L1 pathway. *Front. Immunol.* 11: 624279.
47. Umemura, Y., K. Yamakawa, H. Ogura, H. Yuhara, and S. Fujimi. 2016. Efficacy and safety of anticoagulant therapy in three specific populations with sepsis: a meta-analysis of randomized controlled trials. *J. Thromb. Haemost.* 14: 518–530.
48. Yatabe, T., S. Inoue, S. Sakamoto, Y. Sumi, O. Nishida, K. Hayashida, Y. Hara, T. Fukuda, A. Matsushima, A. Matsuda, et al. 2018. The anticoagulant treatment for sepsis induced disseminated intravascular coagulation; network meta-analysis. *Thromb. Res.* 171: 136–142.
49. Giomarelli, B., V. A. Washington, M. M. Chisholm, L. Quigley, J. B. McMahon, T. Mori, and D. W. McVicar. 2007. Inhibition of thrombin-induced platelet aggregation using human single-chain Fv antibodies specific for TREM-like transcript-1. *Thromb. Haemost.* 97: 955–963.
50. Wolk, K., W. D. Döcke, V. von Baehr, H. D. Volk, and R. Sabat. 2000. Impaired antigen presentation by human monocytes during endotoxin tolerance. *Blood* 96: 218–223.